Mathematical Modeling of Bivariate Polymer Property Distributions Using 2D Probability Generating Functions, 1 – Numerical Inversion Methods

Mariano Asteasuain,* Adriana Brandolin

This is the first of two papers presenting a new mathematical method for modeling bivariate distributions of polymer properties. It is based on the transformation of the infinite mass balances describing the evolution of a two-dimensional distribution using 2D probability generating functions (pgf). A key step of this method is the inversion of the transforms. In this work, two numerical inversion methods of 2D pgfs are developed and carefully validated. The accuracy obtained with both methods was very satisfactory. The inversion formulas of both methods are simple and easy to implement. A simple copolymerization example is used to show the complete procedure from the derivation of the pgf balances to the recovery of the bivariate molecular weight distribution.

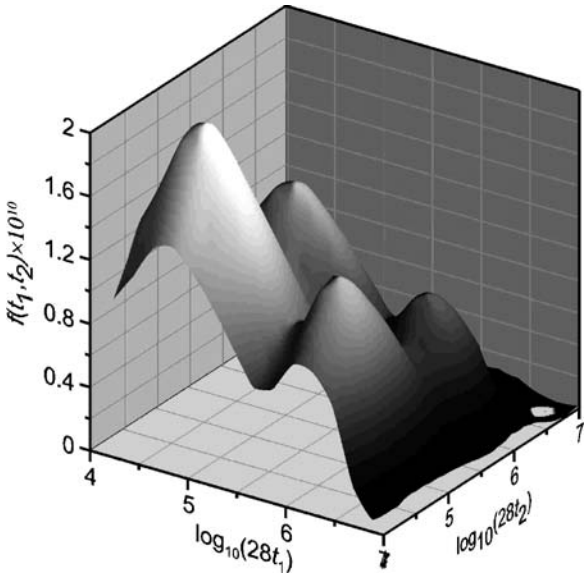

Introduction

The addition of monomer units to form polymer chains in a polymerization process is governed by probabilistic issues which depend on changing process conditions. As a result, the reaction product is composed by a mixture of polymer chains with different size and/or structure. Hence, polymer samples usually present distributions of the different molecular properties, such as molecular weight distribution (MWD), copolymer composition distribution (CCD), short (SCBD) and long (LCBD) chain branching distributions, sequence length distribution (SLD) and particle size distribution (PSD). A detailed knowledge of these distributions is very important because most of the processing and end-use properties of polymers depend on them. For instance, the tensile strength, the glass transition temperature and the melt viscosity of a polymeric material strongly depend on the MWD.[1] Other distributed properties also have great influence on the product quality. Branched polymers, for example, are characterized by the presence of short and/or long chains connected to the main chain. Processing and end-use properties of these polymers

M. Asteasuain, A. Brandolin
Planta Piloto de Ingeniería Química (Universidad Nacional del Sur - CONICET), Camino La Carrindanga km 7, 8000 Bahía Blanca, Argentina
Fax: +54 291 486 1600; E-mail: masteasuain@plapiqui.edu.ar

DOI: 10.1002/mats.200900096

are dependent on the number, type, and distribution of these branches. The LCBD has a strong impact on the rheological behavior of the polymer, affecting the flow properties of the melted polymer (i.e., extensional viscosity, shear viscosity and elasticity), as well as the solid state properties of the material (e.g., orientation effects and stressed induced crystallization).[2] On the other hand, the SCBD determines the polymer density. In the case of copolymers, the CCD is crucial to the mechanical properties of the material. Therefore, for a proper characterization of a polymer sample it should be necessary simultaneous information on more than one distributed property, such as the molecular weight (MW) and copolymer composition (CC) in copolymer systems, or the MW, short-chain branching (SCB), and/or long-chain branching (LCB) in the case of branched polymers. This requirement should be taken into account in the development of advanced mathematical models of polymer systems. For this purpose, a method for the joint modeling of multiple distributions is required.

Simultaneous information of multiple distributions can be represented in a mathematical model by means of multidimensional distributions. Up to now, a variety of methods for the calculation of one-dimensional distributions have been reported. The MWD has been one of the more extensively studied. Works about modeling of other polymer properties distributions, such as the CCD and the PSD, have also been published. However, the prediction of multidimensional distributions is an area of limited development. In some of the reported works in this line, the numerical fractionation technique has been used for predicting the bivariate MW-LCBD.[2] This method consists in dividing the total population of polymer chains into classes according to the number of branches. However, the reconstruction of the MWD at high monomer conversions and high branching content requires a large number of classes in order to reduce approximation errors. This implies increasing the model size and hence the computational load. Ray[3] obtained an analytical solution for the bivariate MWD in living copolymer systems applying Laplace transforms and generating functions. However, this solution requires that certain ratios between propagation constants and monomer concentrations remained constant to be valid. Ray et al. [4] also developed semi analytical Equations for computing the copolymer MWD in free radical copolymerization systems using generating functions. They contemplated most of the commonly accepted kinetic steps, but they did not take into account chain length dependent reaction rates or scission reactions. Besides, the quasi steady state approximation was employed. Another reported approach is the fixed pivot technique, which has been employed for computing MW-CCDs[5] and MW-LCBDs.[6,7] This is a sectional grid method in which the distribution domains are discretized in such a form that any two moments of the distribution in each dimension are exactly preserved.[8] Good quality performance was obtained with this technique, but it requires special computational skills in order to overcome its numerical complexity.[6] The h-p-Galerkin method in combination with border density functions has also been used for modeling bivariate MW-SCBD and MW-LCBD.[9,10] In addition to the deterministic methods described before, statistical tools have also been employed. The well-known Monte Carlo method has been applied to the prediction of MW-CCD[5] and MW-LCBD.[6] Markov chains methods have also been used for the MW-CCD prediction in copolymerization processes.[11] These statistical methods are straightforward techniques that can generally handle complex kinetic mechanisms, but they usually demand significant computational effort.[12]

In this work we present a new approach for the prediction of bivariate distributions of polymer properties, based on the transformation of population mass balances by means of probability generating functions (pgfs). Previously, our research group has perfected the pgf technique as a comprehensive numerical tool for the prediction of the MWD in free radical polymer processes.[13,14] The pgf method was developed as a general modeling tool. It does not assume a priori any shape of the distribution and can be applied to different systems, even those described by complex kinetic mechanisms. It has provided excellent results in terms of accuracy, simplicity of implementation, and computational effort, in models for simulation and optimization activities.[15–21] In its previous state of the art, this technique employed univariate pgfs, which allowed modeling a one-dimensional distribution. Now, we present an extension of this technique to 2D pgfs, in order to model bivariate distributions. As will be explained in detail below, the pgf technique can be divided into two main parts: the transformation of the population mass balances into the pgf domain in order to obtain a set of Equations describing the evolution of the pgf transform of the distribution, and the inversion of the calculated pgf transforms in order to recover the desired distribution. Part I of this work is devoted mainly to the development of suitable numerical inversion methods of 2D pgfs. In addition, a simple copolymerization example is presented for which the pgf balances are derived and solved. The resulting pgfs are numerically inverted with the proposed methods to recover the bivariate MWDs. Work dealing with the detailed algebraic procedures required for the transformation of population balances that commonly appear in several copolymerization systems of different complexity is under way. It will be presented as Part 2 of this series.

pgf Modeling Method

In general, polymer processes can be represented in mathematical terms by a system of population balance Equations of the form $\partial[P(\mathbf{t})]/\partial\tau = f(.)$, in which polymer

Macromol. Theory Simul. **2010**, *19*, 000–000

Macromolecular Journals

DOI: 10.1002/mats.200900096

species P are described by a set **t** of distributed molecular properties. Elements of **t** may be one or more molecular properties such as total chain length, number of comonomer units, short or long branches, etc. Usually, direct solution of these population balances in order to obtain the molecular property distributions (i.e., $P(\mathbf{t})$ for given ranges of each element of **t**) is not feasible because they commonly form a coupled system of Equations in which **t** has to be parameterized for all possible values of each of its elements, which in most of the cases can theoretically vary from one to infinity.

The method presented in this work to tackle this problem in the case of bivariate distributions (i.e., dimension of **t** is two) employs 2D pgf transforms. The 2D pgf transform is defined for a discrete bivariate function $f(t_1,t_2)$ as

$$\hat{\hat{f}}(z1,z2) = \sum_{t_1=1}^{\infty}\sum_{t_2=1}^{\infty} z1^{t_1} z1^{t_2} f(t_1,t_2) \tag{1}$$

where $z1$ and $z2$ are the dummy variables of the pgf, corresponding to the transformation on t_1 and t_2, respectively. The strategy of the pgf modeling method is outlined in Figure 1. This schema is presented for a bivariate distribution, but it holds for any n-dimensional case. The method is based on the transformation of the infinite population mass balances governing the polymer process into the pgf domain, obtaining a system of Equations in which the dependent variable is the pgf transform of the distribution. Pgf values are obtained by solving this system, and they are input to an inversion formula in order to recover the desired distribution. The benefit of this transformation is that only pgf evaluations at a relatively coarse grid of their dummy variables $z1$ and $z2$ are required for recovering the distribution for a set of arbitrary values of its independent variables t_1 and t_2. Hence, a finite and reasonably sized system of Equations needs to be solved.

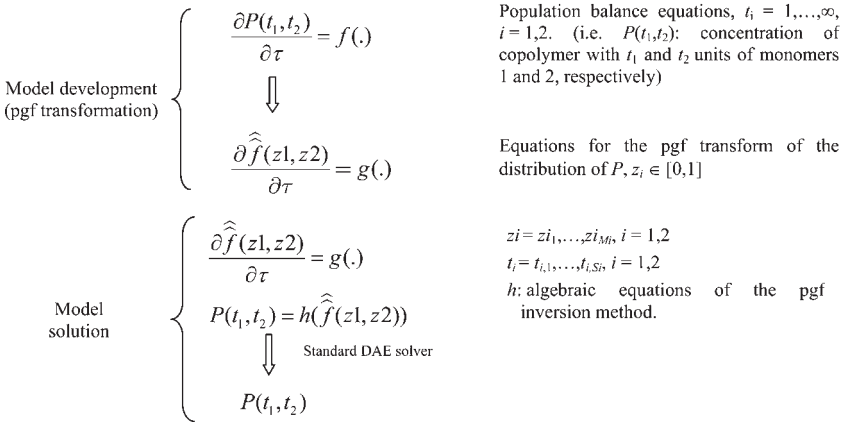

Figure 1. Scheme of the pgf modeling method.

In the following, suitable numerical inversion methods of 2D pgfs are presented and thoroughly analyzed, while Part 2 of this series is devoted to the mathematical procedures required to obtain the transformed equations. This includes the development of a pgf transform table, likewise a Laplace transform table, which allows an easy transformation of the population balance equations.

Numerical Inversion of 2D pgfs

When the 2D pgf $\hat{\hat{f}}(z1,z2)$ can be computed, the original function $f(t_1,t_2)$ can be obtained by means of the double inversion

$$f(t_1,t_2) = \phi^{-2}_{z1,z2}\left\{\hat{\hat{f}}(z1,z2)\right\} \tag{2}$$

A two-step procedure, which was proposed by Valkó and Abated for the 2D Laplace transform inversion,[22] is employed here as a starting point in the development of methods for performing this double inversion of the 2D pgfs. In the first step, z2 is regarded as a constant and the inversion is performed with respect to z1 only:

$$\hat{f}(t_1,z2) = \phi^{-1}_{z1}\left\{\hat{\hat{f}}(z1,z2)\right\} \tag{3}$$

In the second step, $\hat{f}(t_1,z2)$ is inverted with respect to z2 obtaining $f(t_1,t_2)$:

$$f(t_1,t_2) = \phi^{-1}_{z2}\left\{\hat{f}(t_1,z2)\right\} \tag{4}$$

Equation (3) and (4) can be employed in two nested loops in order to perform the inversion: Equation (4) is the outer loop, in which $f(t_1,t_2)$ is formulated as function of $\hat{f}(t_1,z2)$; Equation (3) is the inner loop, in which the required values of $\hat{f}(t_1,z2)$ are formulated as function of $\hat{\hat{f}}(z1,z2)$. Since inversion of univariate pgfs is performed in each one of these steps, it is possible to use inversion algorithms developed for this type of pgf. From our previous works with univariate pgfs, we have developed a variety of well-established methods of this type. In this work two of them, the adaptations to pgf inversion of the methods proposed by Stehfest[23] and Papoulis[14] for

Laplace transforms, were evaluated for the proposed inversion scheme of 2D pgfs. The Stehfest inversion method for univariate pgf consists of the following formula:[23]

$$f(t) = \frac{\ln(2)}{t}\sum_{n=1}^{N} k_n \widehat{f}(z_n) = \frac{\ln(2)}{t}\mathrm{k}^{\mathrm{T}}\widehat{\mathrm{f}}(z) \tag{5}$$

where $\widehat{\mathbf{f}}(\mathbf{z}) = [\widehat{f}(z1),\widehat{f}(z2),\ldots,\widehat{f}(z_N)]^{\mathrm{T}}$ is a vector of univariate pgf transforms evaluated at $z_n = \mathrm{e}^{-n\ln(2)/t}$, N is an even integer, which is a parameter of the method, and k_n ($n = 1,\ldots,N$) are coefficients defined by

$$k_n = (-1)^{n+N/2}\sum_{m=[(n+1)/2]}^{\min(n,N/2)} \times \frac{m^{N/2}(2m)!}{(N/2-m)!m!(m-1)!(n-m)!(2m-n)!} \tag{6}$$

By applying Equation (5) to perform the univariate inversion of the outer loop of the two step procedure, indicated in Equation (4), the following expression is obtained:

$$f(t_1,t_2) = \frac{\ln(2)}{t_2}\mathbf{k}^{\mathrm{T}}\widehat{\mathbf{f}}(t_1,\mathbf{z}2) \tag{7}$$

where $\widehat{\mathbf{f}}(t_1,\mathbf{z}2)$ is a vector of univariate pgf transforms evaluated at $z_{2,j} = \mathrm{e}^{-j\ln(2)/t_2}$. Application of Equation (5) to Equation (7) at each of the elements of $\widehat{\mathbf{f}}(t_1,\mathbf{z}2)$ in order to perform the inner loop inversion with respect to $z1$ [Equation (3)] results in the following expression:

$$f(t_1,t_2) = \frac{(\ln(2))^2}{t_1 t_2}\mathbf{k}^{\mathrm{T}}\widehat{\widehat{\mathbf{f}}}(\mathbf{z}1,\mathbf{z}2)\mathbf{k} \tag{8}$$

where

$$\widehat{\widehat{\mathbf{f}}}(\mathbf{z}1,\mathbf{z}2) = \begin{bmatrix} \widehat{\widehat{f}}(z1_1,z2_1) & \widehat{\widehat{f}}(z1_1,z2_2) & \ldots & \widehat{\widehat{f}}(z1_1,z2_N) \\ \widehat{\widehat{f}}(z1_2,z2_1) & \ldots & \ldots & \widehat{\widehat{f}}(z1_2,z2_N) \\ \vdots & \vdots & \vdots & \vdots \\ \widehat{\widehat{f}}(z1_N,z2_1) & \ldots & \ldots & \widehat{\widehat{f}}(z1_N,z2_N) \end{bmatrix}, \quad zi_j = \mathrm{e}^{-j\ln(2)/t_i} \tag{9}$$

Equation (8), (6) and (9) constitute the 2D pgf inversion formula based on Stehfest method, to which we will refer as the Stehfest 2D pgf inversion formula. It can be seen that the number of pgf evaluations for each pair of values (t_1,t_2) required for this method is

$$n_{\mathrm{ev,Ste}} = N^2 \tag{10}$$

The second univariate pgf inversion technique considered for the 2D pgf inversion is the Papoulis method.[14] The inversion formula of this method is

$$f(t) = \sum_{n=0}^{N} a_n p_{2n}(1/2) = \mathbf{a}^{\mathrm{T}}\mathbf{p}(1/2) \tag{11}$$

where N is an integer number, parameter of the method, $p_{2n}(x)(n = 0,\ldots,N)$ are Legendre polynomials of order $2n$ evaluated at $x = 1/2$ and a_n are the coefficients of the expansion in Legendre polynomials. These polynomials can be computed recursively as follows:

$$\begin{aligned} p_0(x) &= 1 \\ p_1(x) &= x \\ (n+1)p_{n+1}(x) &= (2n+1)xp_n(x) - np_{n-1}(x) \end{aligned} \tag{12}$$

In turn, the coefficients **a** can be obtained by solving the system of equations

$$\mathbf{A}\mathbf{a} = \mathbf{b} \tag{13}$$

where **A** is a lower triangular matrix whose elements are defined as

$$\begin{aligned} A_{k,m} &= \frac{(k-m+1)_m}{2(k+1/2)_{m+1}}\ m = 0,\ldots,k; k \\ &= 0,\ldots,N \text{ where } (j)_l \\ &= \begin{cases} 1 & l = 0 \\ j(j+1)\ldots(j+l-1) & l > 0 \end{cases} \end{aligned} \tag{14}$$

and the elements of **b** are

$$b_i = \frac{\ln(2)}{t}\widehat{f}(z_i),\ z_i = \mathrm{e}^{-(2i+1)\ln(2)/t},\ \ i = 0,\ldots,N \tag{15}$$

Applying Equation (11) in the outer and inner loops of the two step procedure for the 2D pgf inversion, equivalently as was explained before when the Stehfest method was used for obtaining Equation (8), the following expression is obtained

$$f(t_1,t_2) = \frac{(\ln(2))^2}{t_1 t_2}\mathbf{v}^{\mathrm{T}}\widehat{\widehat{\mathbf{f}}}(z1,z2)\mathbf{v} \tag{16}$$

Macromol. Theory Simul. **2010**, *19*, 000–000

DOI: 10.1002/mats.200900096

where

$$\hat{\hat{\mathbf{f}}}(\mathbf{z1},\mathbf{z2}) = \begin{bmatrix} \hat{\hat{f}}(z1_0,z2_0) & \hat{\hat{f}}(z1_0,z2_1) & \dots & \hat{\hat{f}}(z1_0,z2_N) \\ \hat{\hat{f}}(z1_1,z2_0) & \dots & \dots & \hat{\hat{f}}(z1_1,z2_N) \\ \vdots & \vdots & \vdots & \vdots \\ \hat{\hat{f}}(z1_N,z2_0) & \dots & \dots & \hat{\hat{f}}(z1_N,z2_N) \end{bmatrix}, \quad zi_j = e^{-(2j+1)\ln(2)/t_i} \tag{17}$$

and $\mathbf{v}$ can be obtained by solving the linear system

$$\mathbf{A}^T\mathbf{v} = \mathbf{p} \tag{18}$$

Equation (16), (12), (14), (17) and (18) constitute the 2D pgf inversion formula based on the Papoulis method, to which we will refer as the Papoulis 2D pgf inversion formula. The number of pgf evaluations for each pair of values (t_1,t_2) required for this method is

$$n_{ev,Pap} = (N+1)^2 \tag{19}$$

There is a noticeable similitude between the structures of Stehfest and Papoulis inversion formulas. For equivalent values of parameter N in these methods, that is values that lead to the same number of transform evaluations ($N_{Ste} = N_{Pap} + 1$), the difference between both methods is found in the elements of the vectors multiplying $\hat{\hat{f}}(z1,z2)$ and in the values of $z1$ and $z2$ in which the pgfs are evaluated.

Validation of the Numerical Inversion Methods

The performance of Stehfest and Papoulis methods was analyzed by carrying out the inversion of 2D pgfs of known bivariate distribution functions. The functions recovered from the transform domain were compared to the true ones in order to assess the quality of the inversion. Four bivariate distributions that simulated copolymer MWDs were employed. They were built by combining MWDs of actual homopolymers available in our labs. The bivariate MWDs were obtained from the univariate MWDs of the homopolymers in the following way:

$$f(t_1,t_2) = f_1(t_1)f_2(t_2) \tag{20}$$

where $f_i(t_i)$, $i = 1,2$, are two homopolymers MWDs. In this way it is verified that $\sum_{t_1=1}^{\infty}\sum_{t_2=1}^{\infty} f(t_1,t_2) = 1$. Here, and from now on wherever $f(i,j)$ is a MWD, the untransformed variables i and j are degrees of polymerization in each of the comonomers of the polymer in monomer i. The bivariate distributions are shown in Figure 2. As can be seen, they covered a wide spectrum of shapes (simple and complex), widths, and ranges of their independent variables.

To compute the 2D pgfs of these distributions, Equation (21) was employed. This is an adaptation of the 2D pgf definition given in Equation (1) to the experimental data.

$$\hat{\hat{f}}(z1,z2) = \sum_{i=t_{1,1}}^{t_{1,max}}\sum_{j=t_{2,1}}^{t_{2,max}} z1^i z2^j f(i,j) \tag{21}$$

To accomplish the summations indicated in Equation (21) it was necessary to evaluate the distributions beginning at the lowest available degrees of polymeriza-

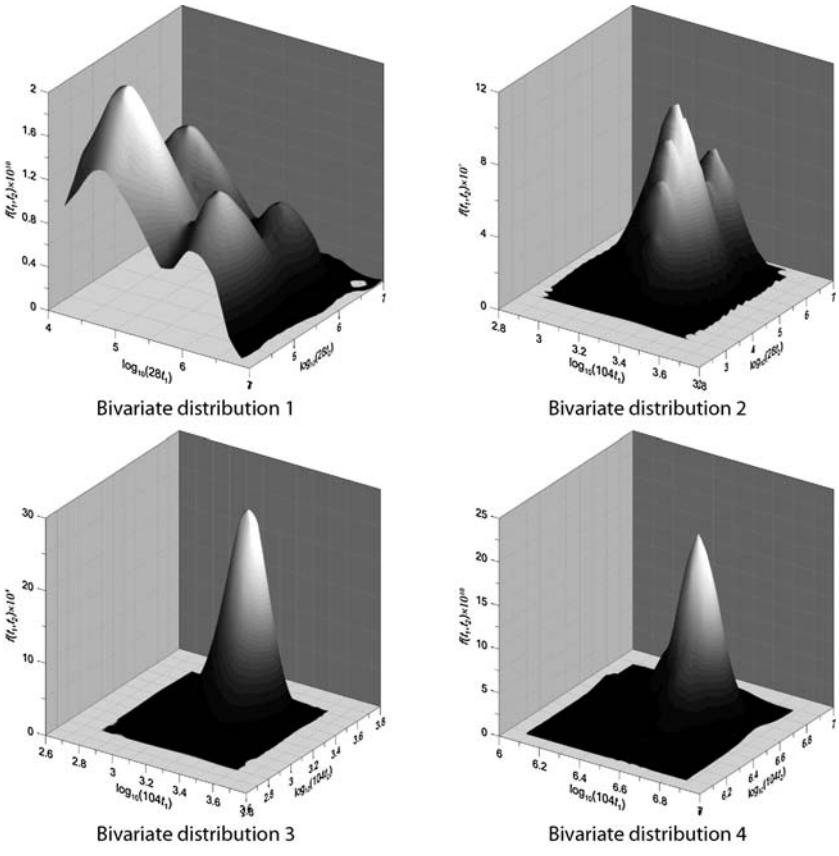

Figure 2. Bivariate distributions obtained from MWDs of actual polymers employed in the validation of the 2D pgf inversion methods.

tions ($t_{k,1}$) and advance with step one up to the maximum degree of polymerization in the experimental data (t_{k,UB_k}). Cubic splines[24] were applied to the experimental data to obtain all the information needed to calculate Equation (21).

In order to quantify the error involved in the recovery of the distributions, the following error function was evaluated:

$$\text{Errel} = \frac{\sum_{i=1}^{I}\sum_{j=1}^{J}\left|f_{\text{rec}}(t_{1,i},t_{2,j}) - f(t_{1,i},t_{2,j})\right|}{f^{\max}IJ} \tag{22}$$

where $f_{\text{rec}}(.)$ and $f(.)$ are the recovered and original distributions, respectively, $t_{1,i}$, $i=1,\ldots,I$ and $t_{2,j}$, $j=1,\ldots,J$ are the values of t_1 and t_2 at which the distribution is being recovered, and $f^{\max}$ is the maximum value of f in the t_1, t_2 domain. The error indicator Errel measures the sum of the absolute errors with respect to the true function, scaled by the maximum value of the latter. This scaling emphasizes the error at the points where the function takes greater values and minimizes the error at the less significant points (e.g., tails of the distribution).

The performance of the inversion methods strongly depends on the value of their parameter N. As N increases, truncation error diminishes but at the same time round-off error becomes larger. Hence, there is a compromise value of the parameter that yields the best possible result, that is, the smallest error with respect to the true function. In our previous works on univariate pgf inversion,[14,23] it was shown that curves obtained with two successive values of N became closer to each other as N increased towards its best value. After that point, they started to separate due to the influence of the increasing round-off error. For this reason, a good criterion for selecting the value of the parameter consisted in performing the inversion repeatedly with increasing values of the parameter, and then choosing the recovered function obtained with the value of N for which the difference between the function recovered with it and the function recovered with the nearest smaller value of the parameter was minimal. The validity of this criterion for the 2D pgf inversion methods was analyzed in this work. The expression shown in Equation (23) was used to measure the difference between the functions recovered with the two values of N:

$$\text{Emet}(N) = \frac{\sum_{i=1}^{I}\sum_{j=1}^{J}\left|f_{\text{rec}}^{N}(t_{1,i},t_{2,j}) - f_{\text{rec}}^{N^-}(t_{1,i},t_{2,j})\right|}{f^{\max}IJ} \tag{23}$$

where $f_{\text{rec}}^{N}(.)$ and $f_{\text{rec}}^{N^-}(.)$ are distributions recovered with two consecutive values of parameter N ($N^- = N-1$ for the Papoulis and $N^- = N-2$ for the Stehfest method).

The Stehfest and Papoulis methods were then used to perform the inversion of the 2D pgfs of the bivariate distributions shown in Figure 2, for a range of values of the methods' parameter. Indicators Errel and Emet(N) were employed to quantify the accuracy of the inversion and the criteria for selecting the value of methods' parameter, respectively.

Recovery of Cumulative Distribution Functions

In addition to mass distribution functions, like the ones previously considered, cumulative distribution functions are also important in polymer science. Given a univariate mass distribution of the form $f(t)$, the cumulative distribution $F(t)$ is defined as

$$F(t) = \sum_{s=0}^{t} f(s) \tag{24}$$

In the case of a bivariate distribution, it is possible to define cumulative distributions with respect to one or to both of the independent variables, i.e.:

$$\begin{aligned} F_{t_1}(t_1,t_2) &= \sum_{s=0}^{t_1} f(s,t_2) \\ F_{t_2}(t_1,t_2) &= \sum_{s=0}^{t_2} f(t_1,s) \\ F_{t_1t_2}(t_1,t_2) &= \sum_{s_1=0}^{t_1}\sum_{s_2=0}^{t_2} f(s_1,s_2) \end{aligned} \tag{25}$$

A conventional way of calculating cumulative distributions is to compute the mass distribution ($f(t_1,t_2)$ in the case of a bivariate distribution) for a grid of values of the function arguments, and then perform the summations interpolating for the values not included in the grid points. However, this grid must be dense enough for this procedure to yield accurate results. On the other hand, the pgf technique allows computing cumulative distributions efficiently from the point of view of the number of function evaluations. This is so because it is possible to obtain the pgf transform of the cumulative distribution $F_*(t_1,t_2)$ defined in Equation (25), and then invert the pgf to obtain the cumulative distribution straightforwardly, without the need of computing a large set of values of the mass distribution. This procedure is a conventional pgf inversion that requires the same amount of calculus as a single mass distribution inversion. In Part 2 of this work it will be demonstrated that there is a relationship between the pgf transform of the mass distribution $f(t_1,t_2)$

Macromol. Theory Simul. **2010**, *19*, 000–000

Macromolecular Journals

DOI: 10.1002/mats.200900096

and the one of the cumulative distribution $F_*(t_1,t_2)$, given by

$$\hat{\hat{F}}_{z_i}(z1,z2) = \frac{\hat{\hat{f}}(z1,z2)}{(1-z_i)}, \quad i=1,2$$
$$\hat{\hat{F}}_{z1z2}(z1,z2) = \frac{\hat{\hat{f}}(z1,z2)}{(1-z1)(1-z2)} \tag{26}$$

where $\hat{\hat{F}}_{z_i}(z1,z2)$ and $\hat{\hat{F}}_{z1z2}(z1,z2)$ are the pgf transforms of $F_{t_i}(t_1,t_2)$ and $F_{t_1t_2}(t_1,t_2)$, respectively. This means that if $\hat{f}(z1,z2)$ is available (e.g., through population balances transformation, or by applying the pgf definition to a known distribution, as described in the previous section), the pgf transform of the cumulative distribution will be readily available.

The 2D pgf inversion methods proposed in this work will be also tested for cumulative distribution inversion.

Application Example

A motivating example of the application of the pgf technique for modeling bivariate distributions is presented in this section. The polymer system is the living copolymerization of styrene and butadiene at 29 °C in benzene with Li^+ counterions.[3] This system was selected because, due to its simplicity, it is easy to follow the method to proceed from the polymerization mechanism, the kinetic rate functions and the derived population balance Equations to the 2D pgf Equations that are solved in the model. For the same reason it is also easy to apply a reference method to validate the results of the pgf technique. However, a comprehensive analysis of the pgf transformation of population balances and solution of more complex case studies will be presented in Part 2 of this work.

Assuming that the initiation step is much faster than the propagation step,[3] the system can be described by the set of mass balances shown in Table 1. Symbols M^i, P_{t_1,t_2}, and Q_{t_1,t_2} denote, respectively, the two monomers ($i=1$ styrene and $i=2$ butadiene), living copolymer with a M^1 final unit and living copolymer with a M^2 final unit; subscripts t_1 and t_2 are, respectively, the number of M^1 and M^2 units in the copolymer chains.

In order to apply the pgf technique to model the copolymer bivariate MWD, the population balances shown in Equation (29) and (30) are transformed into the pgf domain in order to obtain the pgf transforms of the distributions of the polymer species. The transformed equations are shown in Equation (32) and (33) in Table 2.

The pgf transform of a balance Equation is composed by the sum of the transforms of its individual terms. In order to carry out the 2D pgf transformation, each term of the population balance Equation is multiplied by $z1^{t_1}z2^{t_2}$ and then a double summation for all possible values of t_1 and t_2 is performed. The result is expressed in terms of the 2D pgfs that naturally appear in the form of their definitions, obtaining an Equation which is now function of the 2D pgf. In this operation the definition of the double moment of order (*i*,*j*) of the distribution, shown in Equation (31), may appear.

$$\lambda_{i,j} = \sum_{t_1=0}^{\infty}\sum_{t_2=0}^{\infty} t_1^i t_2^j f(t_1,t_2) \tag{31}$$

For instance, for the term $-K_{11}[M^1][P_{t_1,t_2}]$ in Equation (29) the multiplication and double summation lead to

$$-\sum_{t_1=1}^{\infty}\sum_{t_2=0}^{\infty} z1^{t_1}z2^{t_2}K_{11}[M^1][P_{t_1,t_2}] = -K_{11}[M^1]\sum_{t_1=0}^{\infty}\sum_{t_2=0}^{\infty} z1^{t_1}z2^{t_2}[P_{t_1,t_2}] \tag{36}$$

In the previous equation, the sum in t_1 could be extended to $t_1=0$ because the moiety $[P_{0,t_2}]$does not exist in the system, and hence it can be considered $[P_{0,t_2}]=0$. Defining

Table 1. Mass balances of the living copolymerization system.

Species	Equation	
monomer M^1 (styrene)	$\frac{d[M^1]}{dt} = -\left(K_{11}\lambda^{P}_{0,0} + K_{21}\lambda^{Q}_{0,0}\right)[M^1]$	(27)
monomer M^2 (butadiene)	$\frac{d[M^2]}{dt} = -\left(K_{12}\lambda^{P}_{0,0} + K_{22}\lambda^{Q}_{0,0}\right)[M^2]$	(28)
living copolymer with monomer M^1 final unit	$\frac{d[P_{t_1,t_2}]}{dt} = K_{11}[M^1]\left([P_{t_1-1,t_2}](1-\delta_{t_1,1}) - [P_{t_1,t_2}]\right) + K_{21}[M^1]\left[Q_{t_1-1,t_2}\right](1-\delta_{t_1,1}\delta_{t_2,0}) - K_{12}[M^2][P_{t_1,t_2}]$ $t_1 = 1,\ldots,\infty, t_2 = 0,\ldots,\infty \left[P_{t_1,t_2}\right](0) = \delta_{t_1,1}\delta_{t_2,0}[P_0]$	(29)
living copolymer with monomer M^2 final unit	$\frac{d[Q_{t_1,t_2}]}{dt} = K_{22}[M^2]\left([Q_{t_1,t_2-1}](1-\delta_{t_2,1}) - \left[Q_{t_1,t_2}\right]\right) + K_{12}[M^2][P_{t_1,t_2-1}](1-\delta_{t_1,0}\delta_{t_2,1}) - K_{21}[M^1][Q_{t_1,t_2}]$ $t_1 = 0,\ldots,\infty, t_2 = 1,\ldots,\infty \left[Q_{t_1,t_2}\right](0) = \delta_{t_1,0}\delta_{t_2,1}[Q_0]$	(30)

Table 2. Balance Equations of the 2D pgf transforms and zero order moments of the copolymer bivariate distributions.

Species	Equation
pgf transform of the distribution P_{t_1,t_2}	$\frac{d\psi^P(z1,z2)}{dt} = \left[K_{11}[M^1](z1-1) - K_{12}[M^2]\right]\psi^P(z1,z2) + K_{21}[M^1]z1\psi^Q(z1,z2)$ (32)
	$\psi^P(z1,z2)(0) = z1[P_0]$
pgf transform of the distribution Q_{t_1,t_2}	$\frac{d\psi^Q(z1,z2)}{dt} = \left[K_{22}[M^2](z2-1) - K_{21}[M^1]\right]\psi^Q(z1,z2) + K_{12}[M^2]z2\psi^P(z1,z2)$ (33)
	$\psi^Q(z1,z2)(0) = z2[Q_0]$ with $\psi^P(z1,z2) = \lambda^P_{0,0}\widehat{\widehat{f^P}}(z1,z2), \psi^Q(z1,z2) = \lambda^Q_{0,0}\widehat{\widehat{f^Q}}(z1,z2)$
zero-order moment of the distribution P_{t_1,t_2}	$\frac{d\lambda^P_{0,0}}{dt} = K_{21}[M^1]\lambda^Q_{0,0} - K_{12}[M^2]\lambda^P_{0,0}$ (34)
	$\lambda^P_{0,0}(0) = [P_0]$
zero-order moment of the distribution Q_{t_1,t_2}	$\frac{d\lambda^Q_{0,0}}{dt} = -K_{21}[M^1]\lambda^Q_{0,0} + K_{12}[M^2]\lambda^P_{0,0}$ (35)
	$\lambda^Q_{0,0}(0) = [Q_0]$

Table 3. Performance indicators and distribution moments $\lambda_{i,j}$ corresponding to the Papoulis method for bivariate distribution 1.

N	**pgf evaluations per pair (t_1,t_2)**	**Errel**	**Emet(*N*)**	**$\lambda_{i,j}$, (*i*,*j*) = (0,0), (1,0), (0,1), (2,0), (2,1), (2,2)**	
				Inverted funct.	**True funct.**
5	36	0.0201	NA	1.00, 0.67×10^5 0.67×10^5, 0.62×10^{10} 0.43×10^{10}, 0.62×10^{10}	
6	49	0.0118	0.0239	0.95, 0.62×10^5 0.62×10^5, 0.60×10^{10} 0.40×10^{10}, 0.60×10^{10}	
7	64	0.0118	0.0034	0.96, 0.62×10^5 0.62×10^5, 0.59×10^{10} 0.40×10^{10}, 0.59×10^{10}	
8	81	0.0078	0.012	1.00, 0.69×10^5 0.68×10^5, 0.65×10^{10} 0.45×10^{10}, 0.65×10^{10}	
10	121	0.0090	0.0096	0.98, 0.61×10^5 0.61×10^5, 0.56×10^{10} 0.39×10^{10}, 0.56×10^{10}	
11	144	**0.0070**	0.0064	1.00, 0.61×10^5 0.61×10^5, 0.56×10^{10} 0.40×10^{10}, 0.56×10^{10}	0.98, 0.62×10^5 0.62×10^5, 0.56×10^{10} 0.41×10^{10}, 0.56×10^{10}
12	169	0.0204	0.021	1, 0.82×10^5 0.95×10^5, 0.11×10^{11} 0.84×10^{10}, 0.16×10^{11}	

Macromolecular Journals
DOI: 10.1002/mats.200900096

the probability $n^{P}_{t_1,t_2} = \frac{[P_{t_1,t_2}]}{\sum_{t_1=0}^{\infty}\sum_{t_2=0}^{\infty}[P_{t_1,t_2}]} = \frac{[P_{t_1,t_2}]}{\lambda^{P}_{0,0}}$, which is the number fraction of $[P_{t_1,t_2}]$ with respect to the total amount of P molecules, and substituting in Equation (36), the following expression is obtained:

$$-K_{11}[M^1]\lambda^{P}_{0,0}\sum_{t_1=0}^{\infty}\sum_{t_2=0}^{\infty} z1^{t_1}z2^{t_2}n^{P}_{t_1,t_2} \tag{37}$$

According to the 2D pgf definition given in Equation (1), the double sum $\sum_{t_1=0}^{\infty}\sum_{t_2=0}^{\infty} z1^{t_1}z2^{t_2}n^{P}_{t_1,t_2}$ is the 2D pgf transform of $n^{P}_{t_1,t2}$, and hence the final transformed term is:

$$-K_{11}[M^1]\lambda^{P}_{0,0}\widehat{\widehat{f^{P}}}(z1,z2) = -K_{11}[M^1]\psi^{P}(z1,z2) \tag{38}$$

In the case of the term $K_{11}[M^1][P_{t_1-1,t_2}](1-\delta_{t_1,1})$, the transformation starts with

$$\begin{aligned}&\sum_{t_1=1}^{\infty}\sum_{t_2=0}^{\infty} z1^{t_1}z2^{t_2}K_{11}[M^1][P_{t_1-1,t_2}](1-\delta_{t_1,1})\\ &\quad = K_{11}[M^1]\sum_{t_1=2}^{\infty}\sum_{t_2=0}^{\infty} z1^{t_1}z2^{t_2}[P_{t_1-1,t_2}]\end{aligned} \tag{39}$$

Taking $t_1-1=s$ and replacing in Equation (39),

$$\begin{aligned}&K_{11}[M^1]\sum_{s=1}^{\infty}\sum_{t_2=0}^{\infty} z1^{s+1}z2^{t_2}[P_{s,t_2}]\\ &\quad = K_{11}[M^1]z1\sum_{s=2}^{\infty}\sum_{t_2=0}^{\infty} z1^{s}z2^{t_2}[P_{s,t_2}]\end{aligned} \tag{40}$$

Taking $[P_{0,t_2}]=0$ and extending the sum in s to $s=0$ the final transformed term is obtained:

$$\begin{aligned}&K_{11}[M^1]\,z1\sum_{s=0}^{\infty}\sum_{t_2=0}^{\infty} z1^{s}z2^{t_2}[P_{s,t_2}]\\ &\quad = K_{11}[M^1]z1\psi^{P}(z1,z2)\end{aligned} \tag{41}$$

The initial condition is transformed as well:

$$\sum_{t_1=0}^{\infty}\sum_{t_2=0}^{\infty} z1^{t_1}z1^{t_2}\delta_{t_1,1}\delta_{t_2,0}[P_0] = z1[P_0] \tag{42}$$

The remaining terms of the population balances can be transformed following any of the previous procedures.

Balance Equations for the zero order moments of the distributions of P and Q ($\lambda^{P}_{0,0}$ and $\lambda^{Q}_{0,0}$) are needed to solve the monomer mass balances. The moments' balances

Table 4. Performance indicators and distribution moments $\lambda_{i,j}$ corresponding to the Papoulis method for bivariate distribution 2.

N	**pgf evaluations per pair (t_1,t_2)**	**Errel**	**Emet(N)**	**$\lambda_{i,j}$, (i,j) = (0,0), (1,0), (0,1), (2,0), (2,1), (2,2)**	
				Inverted funct.	**True funct.**
8	81	0.0230	NA	$1.00,\ 0.22\times10^{2}$ $0.66\times10^{5},\ 0.51\times10^{3}$ $0.14\times10^{7},\ 0.58\times10^{10}$	
9	100	0.0155	0.0201	$0.98,\ 0.21\times10^{2}$ $0.60\times10^{5},\ 0.46\times10^{3}$ $0.13\times10^{7},\ 0.51\times10^{10}$	
11	121	0.0099	0.0075	$1.00,\ 0.21\times10^{2}$ $0.62\times10^{5},\ 0.46\times10^{3}$ $0.13\times10^{7},\ 0.54\times10^{10}$	$0.98,\ 0.21\times10^{2}$ $0.60\times10^{5},\ 0.46\times10^{3}$ $0.13\times10^{7},\ 0.52\times10^{10}$
12	169	**0.0086**	0.0126	$0.97,\ 0.20\times10^{2}$ $0.59\times10^{5},\ 0.45\times10^{3}$ $0.12\times10^{7},\ 0.51\times10^{10}$	
13	196	0.0219	0.0142	$0.98,\ 0.20\times10^{2}$ $0.60\times10^{5},\ 0.45\times10^{3}$ $0.13\times10^{7},\ 0.54\times10^{10}$	
14	225	0.0429	0.0564	$1.40,\ 0.33\times10^{2}$ $0.12\times10^{5},\ 0.87\times10^{3}$ $0.32\times10^{7},\ 0.17\times10^{10}$	

can be obtained from Equation (29) and (30) using well-known techniques. The resulting Equations are also shown in Table 2. The mathematical model of the process consists of a DAE system including Equation (32) and (33) parameterized for the set of values of z1 and z2 required by the inversion method, which is function of the parameter N and the set of values of t_1 and t_2 for which the MWD is to be computed. In addition, balances for the monomers and zero order moments of the copolymer MWDs, and the algebraic Equations of the pgf inversion method are also part of the model. In view of the results shown in the next section, the Papoulis inversion method was adopted.

Table 5. Performance indicators and distribution moments $\lambda_{i,j}$ corresponding to the Papoulis method for bivariate distribution 3.

N	pgf evaluations per pair (t_1,t_2)	Errel	Emet(N)	$\lambda_{i,j}$, $(i,j) = (0,0), (1,0), (0,1), (2,0), (2,1), (2,2)$	
				Inverted funct.	True funct.
6	49	0.0385	NA	$1.00, 0.24 \times 10^2$ $0.24 \times 10^2, 0.57 \times 10^3$ $0.53 \times 10^3, 0.57 \times 10^3$	
7	64	0.0395	0.0069	$1.00, 0.23 \times 10^2$ $0.23 \times 10^2, 0.54 \times 10^3$ $0.51 \times 10^3, 0.54 \times 10^3$	
8	81	0.0268	0.0161	$1.00, 0.23 \times 10^2$ $0.23 \times 10^2, 0.52 \times 10^3$ $0.49 \times 10^3, 0.52 \times 10^3$	
9	100	0.0192	0.0260	$1.00, 0.21 \times 10^2$ $0.21 \times 10^2, 0.48 \times 10^3$ $0.45 \times 10^3, 0.48 \times 10^3$	
10	121	0.0220	0.0053	$1.00, 0.21 \times 10^2$ $0.21 \times 10^2, 0.48 \times 10^3$ $0.45 \times 10^3, 0.48 \times 10^3$	
11	144	0.0118	0.013	$1.00, 0.21 \times 10^2$ $0.21 \times 10^2, 0.46 \times 10^3$ $0.43 \times 10^3, 0.46 \times 10^3$	
12	169	0.0078	0.0132	$0.98, 0.20 \times 10^2$ $0.20 \times 10^2, 0.45 \times 10^3$ $0.43 \times 10^3, 0.45 \times 10^3$	
13	196	0.0085	0.0017	$0.99, 0.21 \times 10^2$ $0.21 \times 10^2, 0.45 \times 10^3$ $0.43 \times 10^3, 0.45 \times 10^3$	$0.99, 0.21 \times 10^2$ $0.21 \times 10^2, 0.46 \times 10^3$ $0.43 \times 10^3, 0.46 \times 10^3$
14	225	**0.0054**	0.0039	$0.98, 0.20 \times 10^2$ $0.20 \times 10^2, 0.45 \times 10^3$ $0.43 \times 10^3, 0.45 \times 10^3$	
15	256	0.0118	0.0138	$1.00, 0.25 \times 10^3$ $0.25 \times 10^3, 0.61 \times 10^3$ $0.58 \times 10^3, 0.61 \times 10^3$	
16	289	0.0294	0.0184	$1.49, 0.38 \times 10^2$ $0.38 \times 10^2, 0.10 \times 10^4$ $0.10 \times 10^4, 0.10 \times 10^4$	
17	324	0.314	0.3122	$5.88, 0.17 \times 10^3$ $0.17 \times 10^3, 0.51 \times 10^4$ $0.48 \times 10^4, 0.49 \times 10^4$	

Macromolecular Journals
DOI: 10.1002/mats.200900096

Results and Discussion

Numerical Inversion Methods

Table 3–6 show the performance indicators for Papoulis method. Highlighted in bold are the values of the parameter N that yielded the lowest Errel (best inversion) and underlined the ones corresponding to the minimum Emet(N) (selected values according to the proposed criteria), and the corresponding values of Errel and Emet(N). The values of N for which the inversions were performed for the different distributions were chosen aiming at locating the minimums Errel and Emet(N) by

Table 6. Performance indicators and distribution moments $\lambda_{i,j}$ corresponding to the Papoulis method for bivariate distribution 4.

N	pgf evaluations per pair (t_1,t_2)	Errel	Emet(N)	$\lambda_{i,j}$, (i,j) = (0,0), (1,0), (0,1), (2,0), (2,1), (2,2)	
				Inverted funct.	True funct.
5	36	0.0537	NA	1.22, 0.51×10^5 0.51×10^5, 0.24×10^{10} 0.21×10^{10}, 0.24×10^{10}	
6	49	0.0423	0.0382	1.09, 0.44×10^5 0.44×10^5, 0.19×10^{10} 0.18×10^{10}, 0.19×10^{10}	
7	64	0.0433	0.0251	0.11, 0.43×10^5 0.43×10^5, 0.19×10^{10} 0.17×10^{10}, 0.19×10^{10}	
8	81	0.0332	0.0155	1.06, 0.42×10^5 0.42×10^5, 0.18×10^{10} 0.17×10^{10}, 0.18×10^{10}	
9	100	0.0243	0.0251	1.01, 0.39×10^5 0.39×10^5, 0.16×10^{10} 0.15×10^{10}, 0.16×10^{10}	
10	121	0.0268	0.0054	1.01, 0.39×10^5 0.39×10^5, 0.16×10^{10} 0.15×10^{10}, 0.16×10^{10}	
11	144	0.0194	0.0130	0.98, 0.38×10^5 0.38×10^5, 0.15×10^{10} 0.15×10^{10}, 0.15×10^{10}	
12	169	0.0161	0.0133	0.96, 0.37×10^5 0.37×10^5, 0.15×10^{10} 0.14×10^{10}, 0.15×10^{10}	
13	196	0.0169	0.0024	0.97, 0.37×10^5 0.37×10^5, 0.15×10^{10} 0.14×10^{10}, 0.15×10^{10}	0.98, 0.39×10^5 0.39×10^5, 0.16×10^{10} 0.15×10^{10}, 0.16×10^{10}
14	225	**0.0131**	0.0059	0.97, 0.37×10^5 0.37×10^5, 0.15×10^{10} 0.14×10^{10}, 0.15×10^{10}	
15	256	0.0169	0.0125	1.08, 0.44×10^5 0.44×10^5, 0.20×10^{10} 0.19×10^{10}, 0.20×10^{10}	
16	289	0.0350	0.0199	1.44, 0.67×10^5 0.68×10^5, 0.35×10^{10} 0.33×10^{10}, 0.34×10^{10}	

an inspection procedure. Hence, they do not necessarily coincide.

It can be seen in Table 3–6 that the value of the parameter N that would be selected with the minimum Emet(N) criteria is generally near the one that gives the smallest error with respect to the true distribution (minimum Errel). Only in the case of the bivariate distribution 1 (Table 3) the value of N corresponding to the minimum Emet(N), $N=7$, is far from the one corresponding to the minimum Errel, $N=11$. However, there is another local minimum for Emet(N) at $N=11$ which coincides with the minimum Errel value. Taking into account the previous explanation about the influence of the parameter, it is convenient to use the highest possible value of N. Therefore, it is appropriate to use the latter value of N as it corresponds to the highest value prior that round-off error causes that the recovered distributions start to separate from each other.

The double moments of the bivariate distributions, as defined in Equation (31), of orders $(i,j)=(0,0)$, (1,0), (0,1), (2,0), (1,1), and (0,2) were calculated using both the inverted and true functions. These data are also reported in Table 3–6. It can be seen that the moments obtained with the true distributions compare well with the ones obtained with the inverted distributions corresponding to the minimum Emet(N) criteria. For this case, the summation of the quadratic relative errors of the moment calculation was one of the lowest, showing the goodness of the Emet(N) criteria.

Figure 3–6 show the distributions recovered with the Papoulis method parameterized for some of the computed values of t_1, compared with the true distributions. These curves correspond to the ones recovered with the minimum Emet(N) criteria value of N. In the cases in which this value did not coincide with the one yielding the minimum Errel (actual best value of N), the curves obtained with the latter are also shown. It can be observed that the recovered functions compare well with the true ones in all cases. In particular, it can be noticed that for the cases where the minimum Emet(N) and minimum Errel values of N do not coincide, there is not a visible worsening of the solution with the proposed criteria for the selection of the parameter.

Table 7–10 show the performance indicators corresponding to the Stehfest method. For this method, the

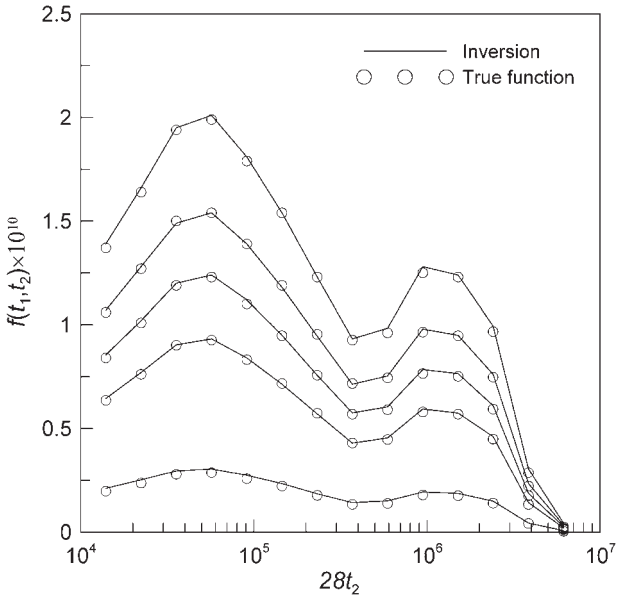

Figure 3. Inversion of the bivariate distribution 1 with the Papoulis method with $N=11$.

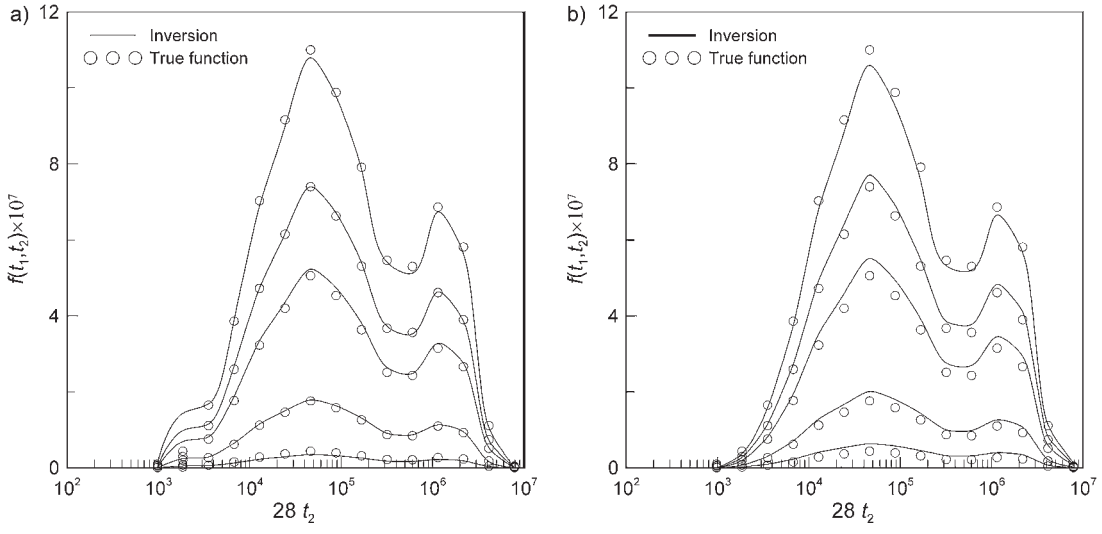

Figure 4. Inversion of the bivariate distribution 2 with the Papoulis method with (a) $N=12$ (minimum Errel), (b) $N=11$ [minimum Emet(N)].

DOI: 10.1002/mats.200900096

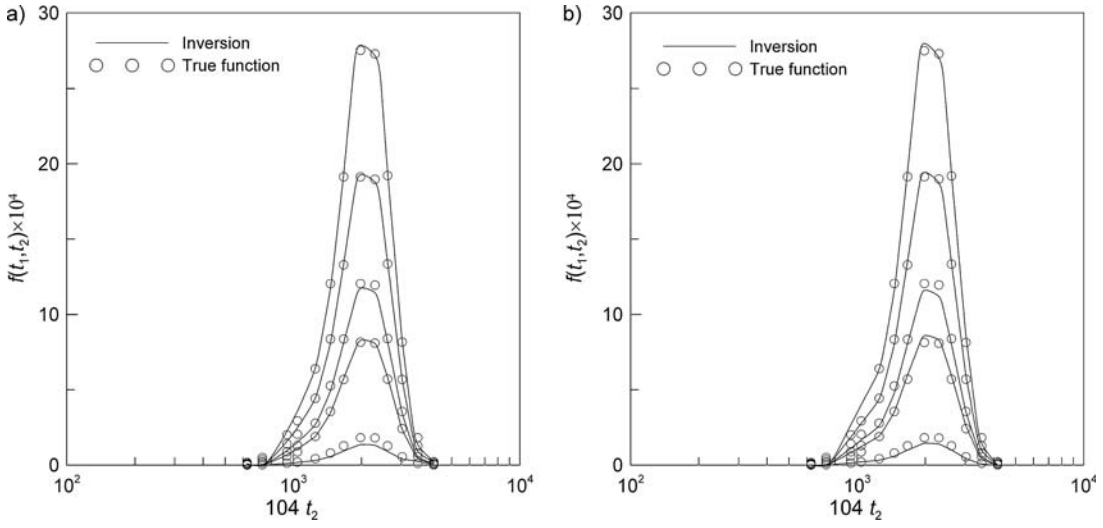

Figure 5. Inversion of the bivariate distribution 3 with the Papoulis method with (a) $N = 14$ (minimum Errel), (b) $N = 13$ [minimum Emet(N)].

values of N resulting from the minimum Emet(N) criteria coincide in all cases with the ones corresponding to the minimum Errel and a good approximation of the distribution moments is obtained. However, the inversion with this method was less accurate than with Papoulis method, as can be seen by comparing the values of Errel for the selected N in each of them. The better performance of the Papoulis method can be corroborated graphically comparing Figure 7–10, which show the plots of the distributions recovered with the Stehfest method, with Figure 3–6 which show the ones obtained with the Papoulis method.

The 2D pgf inversion technique was then applied to the inversion of cumulative distributions. The particular problem considered here involves the representation of bivariate distributions, but the approach can be used in any other application of cumulative distributions. It is common to plot bivariate distributions in two dimension plots, parameterizing one of the function arguments, like in the plots presented previously. In this procedure, information about the not reported values of the parameterized variable is lost. One way of overcoming this inconvenient is to parameterize one of the variables in cumulative intervals, instead of point values. For instance, reporting $F_{t_1}(t_1, t_2)$ vs. t_2 for different values of t_1. Figure 11(a) shows this plot for bivariate distribution 3. In view of the previous results, only the Papoulis method was applied. It can be seen that an excellent accuracy

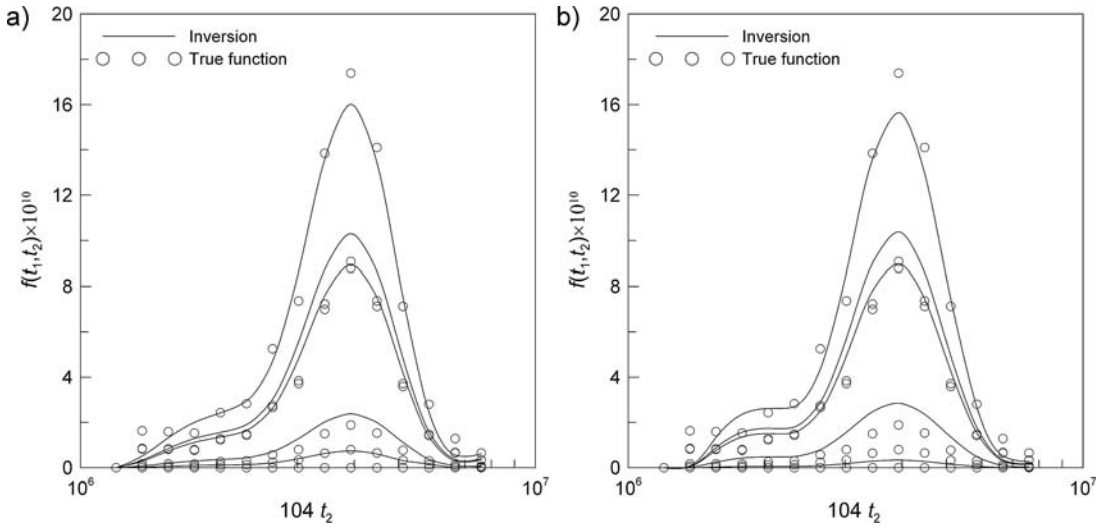

Figure 6. Inversion of the bivariate distribution 4 with the Papoulis method with (a) $N = 14$ (minimum Errel), (b) $N = 13$ [minimum Emet(N)].

Table 7. Performance indicators and distribution moments $\lambda_{i,j}$ corresponding to the Stehfest method for bivariate distribution 1.

N	pgf evaluations per pair (t_1,t_2)	Errel	Emet(*N*)	$\lambda_{i,j}$, (*i*,*j*) = (0,0), (1,0), (0,1), (2,0), (2,1), (2,2)	
				Inverted funct.	True funct.
6	36	0.0130	NA	$0.99, 0.64 \times 10^5$ $0.64 \times 10^5, 0.62 \times 10^{10}$ $0.42 \times 10^{10}, 0.62 \times 10^{10}$	
8	64	0.0079	0.0067	$1.00, 0.64 \times 10^5$ $0.64 \times 10^5, 0.59 \times 10^{10}$ $0.41 \times 10^{10}, 0.59 \times 10^{10}$	
10	100	0.0055	0.0030	$1.00, 0.63 \times 10^5$ $0.63 \times 10^5, 0.58 \times 10^{10}$ $0.42 \times 10^{10}, 0.58 \times 10^{10}$	
12	144	**0.0040**	0.0018	$1.00, 0.64 \times 10^5$ $0.64 \times 10^5, 0.57 \times 10^{10}$ $0.41 \times 10^{10}, 0.57 \times 10^{10}$	$0.98, 0.62 \times 10^5$ $0.62 \times 10^5, 0.56 \times 10^{10}$ $0.41 \times 10^{10}, 0.56 \times 10^{10}$
14	196	0.0145	0.0127	$1.16, 0.15 \times 10^6$ $0.14 \times 10^6, 0.21 \times 10^{11}$ $0.18 \times 10^{11}, 0.21 \times 10^{11}$	
16	256	4.082	4.082	$0.15 \times 10^3, 0.23 \times 10^8$ $0.23 \times 10^8, 0.45 \times 10^{13}$ $0.38 \times 10^{13}, 0.44 \times 10^{13}$	

Table 8. Performance indicators and distribution moments $\lambda_{i,j}$ corresponding to the Stehfest method for bivariate distribution 2.

N	pgf evaluations per pair (t_1,t_2)	Errel	Emet(*N*)	$\lambda_{i,j}$, (*i*,*j*) = (0,0), (1,0), (0,1), (2,0), (2,1), (2,2)	
				Inverted funct.	True funct.
6	36	0.0822	NA	$0.96, 0.21 \times 10^2$ $0.62 \times 10^5, 0.50 \times 10^3$ $0.13 \times 10^7, 0.60 \times 10^{10}$	
8	64	0.0602	0.0321	$1.01, 0.22 \times 10^2$ $0.64 \times 10^5, 0.54 \times 10^3$ $0.14 \times 10^7, 0.58 \times 10^{10}$	
10	100	0.0415	0.0231	$1.03, 0.22 \times 10^2$ $0.64 \times 10^5, 0.54 \times 10^3$ $0.14 \times 10^7, 0.57 \times 10^{10}$	
12	144	0.0286	0.0175	$1.02, 0.22 \times 10^2$ $0.63 \times 10^5, 0.52 \times 10^3$ $0.14 \times 10^7, 0.56 \times 10^{10}$	
14	196	**0.0198**	0.0113	$1.02, 0.22 \times 10^2$ $0.63 \times 10^5, 0.51 \times 10^3$ $0.14 \times 10^7, 0.56 \times 10^{10}$	$0.98, 0.21 \times 10^2$ $0.60 \times 10^5, 0.46 \times 10^3$ $0.13 \times 10^7, 0.52 \times 10^{10}$
16	256	0.1990	0.1971	$0.50 \times 10^1, 0.15 \times 10^3$ $0.57 \times 10^6, 0.46 \times 10^4$ $0.18 \times 10^8, 0.96 \times 10^{11}$	

Macromolecular Journals
DOI: 10.1002/mats.200900096

Table 9. Performance indicators and distribution moments $\lambda_{i,j}$ corresponding to Stehfest method for bivariate distribution 3.

N	**pgf evaluations per pair (t_1,t_2)**	**Errel**	**Emet(N)**	**$\lambda_{i,j}$, (i,j) = (0,0), (1,0), (0,1), (2,0), (2,1), (2,2)**	
				Inverted funct.	**True funct.**
8	64	0.0639	NA	$0.95, 0.21 \times 10^2$ $0.21 \times 10^2, 0.50 \times 10^3$ $0.45 \times 10^3, 0.50 \times 10^3$	
10	100	0.0495	0.0321	$0.98, 0.21 \times 10^2$ $0.21 \times 10^2, 0.50 \times 10^3$ $0.46 \times 10^3, 0.50 \times 10^3$	
12	144	0.0426	0.0207	$0.97, 0.21 \times 10^2$ $0.21 \times 10^2, 0.49 \times 10^3$ $0.45 \times 10^3, 0.49 \times 10^3$	
14	196	**0.0361**	0.0111	$0.95, 0.20 \times 10^2$ $0.20 \times 10^2, 0.46 \times 10^3$ $0.43 \times 10^3, 0.46 \times 10^3$	$0.99, 0.21 \times 10^2$ $0.21 \times 10^2, 0.46 \times 10^3$ $0.43 \times 10^3, 0.46 \times 10^3$
16	256	0.0682	0.0520	$0.14 \times 10^1, 0.33 \times 10^2$ $0.33 \times 10^2, 0.83 \times 10^3$ $0.78 \times 10^3, 0.85 \times 10^3$	
18	324	9.790	9.790	$0.27 \times 10^2, 0.78 \times 10^3$ $0.76 \times 10^3, 0.22 \times 10^5$ $0.23 \times 10^5, 0.23 \times 10^5$	

Table 10. Performance indicators and distribution moments $\lambda_{i,j}$ corresponding to Stehfest method for bivariate distribution 4.

N	**pgf evaluations per pair (t_1,t_2)**	**Errel**	**Emet(N)**	**$\lambda_{i,j}$, (i,j) = (0,0), (1,0), (0,1), (2,0), (2,1), (2,2)**	
				Inverted funct.	**True funct.**
8	64	0.0556	NA	$1.01, 0.41 \times 10^5$ $0.41 \times 10^5, 0.18 \times 10^{10}$ $0.17 \times 10^{10}, 0.18 \times 10^{10}$	
10	100	0.0460	0.0226	$1.05, 0.43 \times 10^5$ $0.43 \times 10^5, 0.19 \times 10^{10}$ $0.17 \times 10^{10}, 0.19 \times 10^{10}$	
12	144	0.0364	0.0173	$1.05, 0.42 \times 10^5$ $0.42 \times 10^5, 0.189 \times 10^{10}$ $0.17 \times 10^{10}, 0.18 \times 10^{10}$	
14	196	**0.0297**	0.0128	$1.04, 0.41 \times 10^5$ $0.41 \times 10^5, 0.17 \times 10^{10}$ $0.16 \times 10^{10}, 0.17 \times 10^{10}$	$0.98, 0.39 \times 10^5$ $0.39 \times 10^5, 0.16 \times 10^{10}$ $0.15 \times 10^{10}, 0.16 \times 10^{10}$
16	256	0.0313	0.0144	$1.16, 0.49 \times 10^5$ $0.49 \times 10^5, 0.22 \times 10^{10}$ $0.21 \times 10^{10}, 0.22 \times 10^{10}$	
18	324	0.7989	0.7927	$5.35, 0.31 \times 10^6$ $0.31 \times 10^6, 0.19 \times 10^{11}$ $0.19 \times 10^{11}, 0.20 \times 10^{11}$	

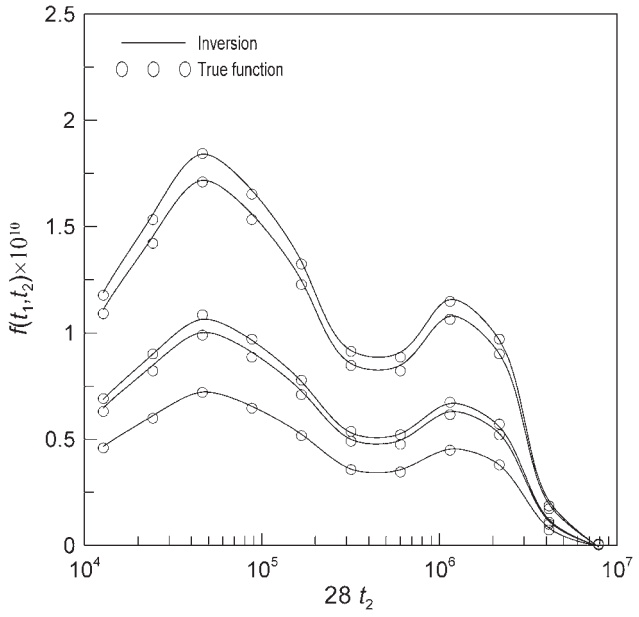

Figure 7. Inversion of the bivariate distribution 1 with the Stehfest method with $N = 12$.

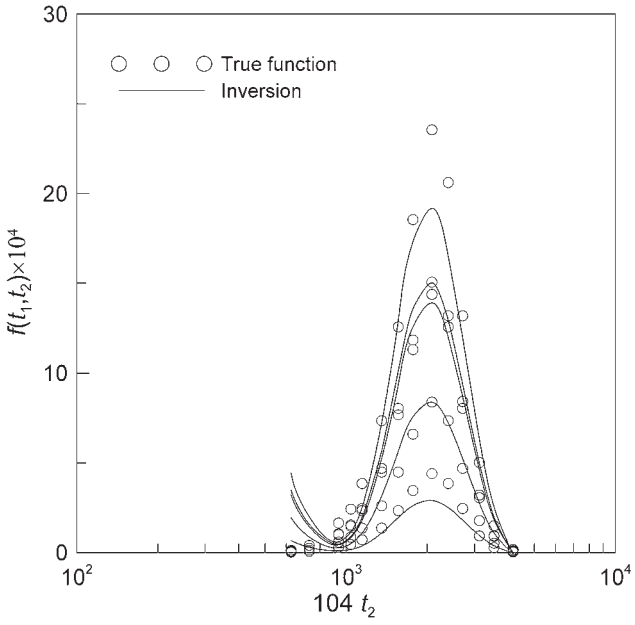

Figure 9. Inversion of the bivariate distribution 3 with the Stehfest method with $N = 14$.

in the inversion was achieved. Similar results were obtained for the other distributions. It should be remarked that, as was mentioned before, no expensive computations of the mass distribution $f(t_1, t_2)$ was necessary in order to calculate $F_{t_1}(t_1, t_2)$, because the latter was recovered from its own pgf transform. Besides, the data on $F_{t_1}(t_1, t_2)$ can be used to obtain plots of the distribution parameterized in mutually excluding intervals of t_1, as is shown in Figure 11(b). For this case, only the recovered function was plotted because this function was simply obtained by subtractions of the cumulative distributions of Figure 11.

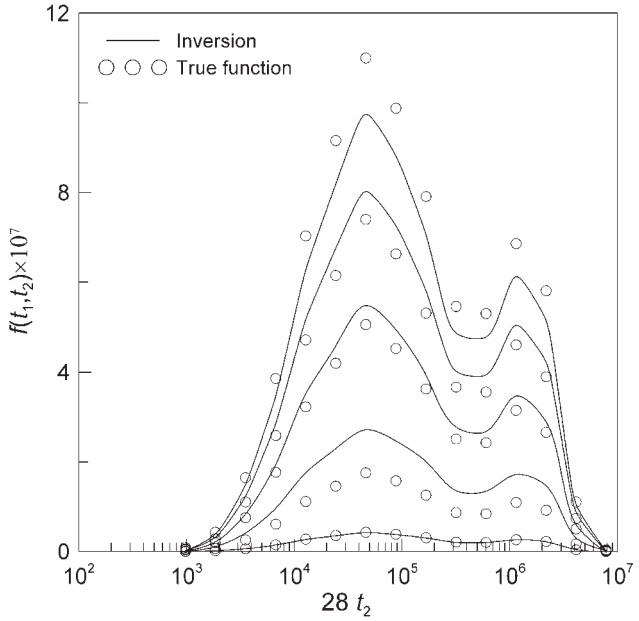

Figure 8. Inversion of the bivariate distribution 2 with the Stehfest method with $N = 14$.

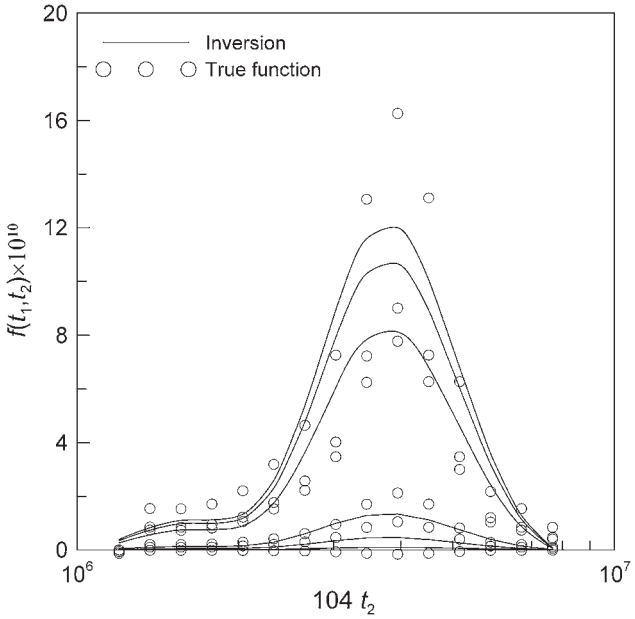

Figure 10. Inversion of the bivariate distribution 4 with the Stehfest method with $N = 14$.

DOI: 10.1002/mats.200900096

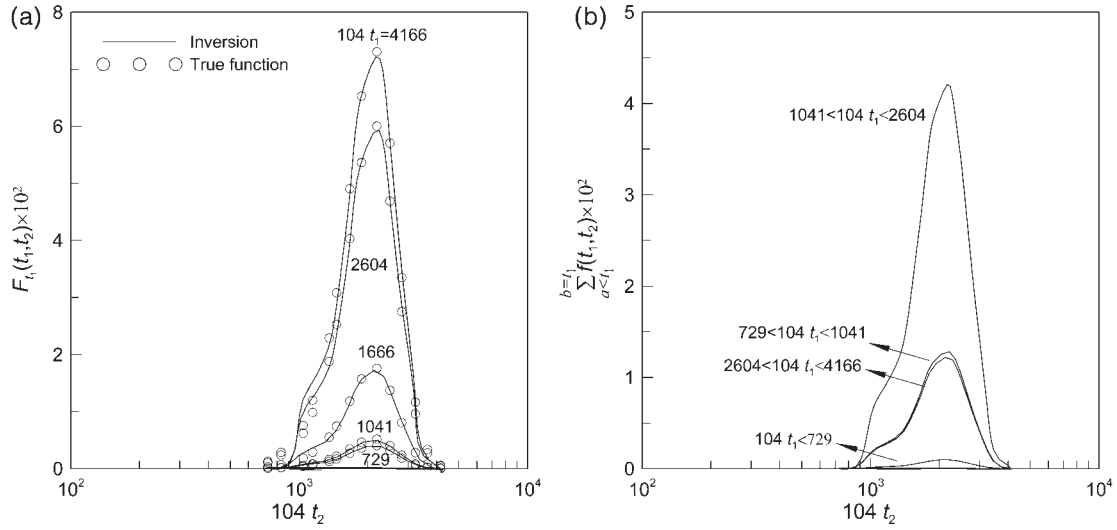

Figure 11. Inversion of the bivariate distribution 3 with the Papoulis method parameterized in (a) cumulative intervals of t_1, (b) mutually excluding intervals of t_1. Value of the parameter $N = 14$.

Application Example

The mathematical model for the application example was solved using the following kinetic parameters:[3] $K_{11} = 0.06\ \mathrm{L\cdot mol^{-1}\cdot s^{-1}}$, $K_{12} = 1.2\ \mathrm{L\cdot mol^{-1}\cdot s^{-1}}$, $K_{21} = 0.006\ \mathrm{L\cdot mol^{-1}\cdot s^{-1}}$ and $K_{22} = 0.018\ \mathrm{L\cdot mol^{-1}\cdot s^{-1}}$, and initial conditions $[M^1](0) = [M^2](0) = 0.5\ \mathrm{mol\cdot L^{-1}}$ and $[P_0](0) = [Q_0](0) = 0.001\ \mathrm{mol\cdot L^{-1}}$. The bivariate distributions computed by the pgf technique were validated by comparison with the ones obtained by direct integration of the original population balances shown in Equation (29) and (30). It should be remarked that direct integration is infeasible in the majority of the polymer systems due to the extremely large number of Equations to be solved. In this case, the simplicity of the population balances and the relatively low molecular weight of the system make possible the direct solution of the population balances. The results are shown in Figure 12 and 13. It can be observed that a very good prediction of the bivariate distributions is obtained with

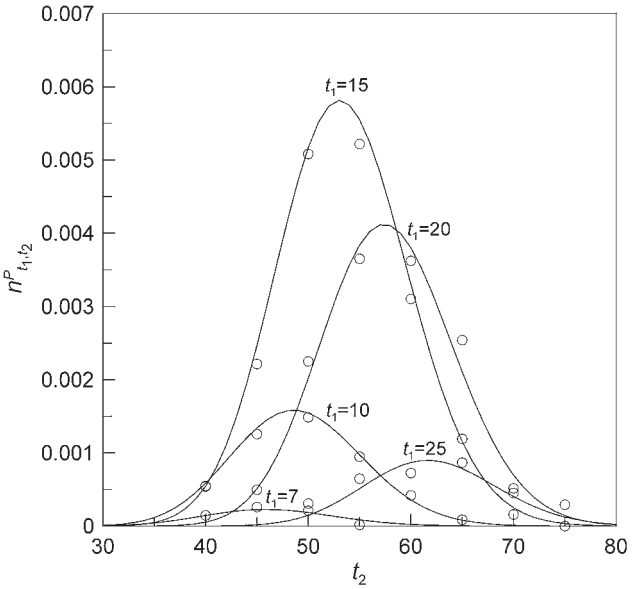

Figure 12. Bivariate molecular weight distribution of the living copolymer with a styrene final unit at a reaction time of 1.4 h. Lines: direct integration; symbols: pgf method.

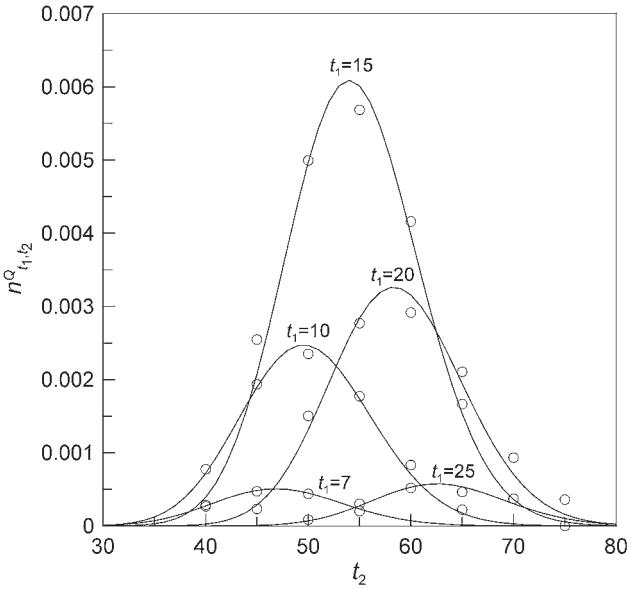

Figure 13. Bivariate molecular weight distribution of the living copolymer with a butadiene final unit at a reaction time of 1.4 h. Lines: direct integration; symbols: pgf method.

the pgf technique coupled with the inversion method proposed in this work.

Conclusion

This is the first part of a work in which a mathematical method for modeling bivariate distributions of polymer properties using 2D pgf transforms is presented. The pgf method was developed as a general modeling tool that can be applied to model diverse types of bivariate distributions in different systems described by a set of population mass balances. The method is based on the transformation of the population mass balances into the 2D pgf domain, solution of the finite set of transformed Equations and numerical inversion of the pgf transforms in order to recover the bivariate distribution.

The inversion of the pgf in order to recover the distribution is a key step of this method. In this part of the work, two numerical methods, the Papoulis and Stehfest methods, were developed for the inversion of the 2D pgfs. A careful validation of these methods was performed comparing known distributions with the ones inverted from their 2D pgf transforms. For this purpose, bivariate distributions were generated from MWDs of actual polymers, covering a very wide range of shapes. As part of the validation process, techniques for setting the value of the methods' parameters were developed. The accuracy in the inversion obtained with both methods was very satisfactory. However, the Papoulis method showed less sensitivity to round-off error and better exactitude. The inversion formulas of both methods are very simple and easy to implement.

The pgf technique coupled with the inversion method proposed in this work shows a great potential for modeling bivariate population distributions as shown by the results obtained for the living copolymerization of styrene and butadiene.

Part 2 of this work will address the mathematical procedures required to obtain the transformed equations. This includes the development of a pgf transform table, likewise a Laplace transform table, which allows an easy transformation of the population balance equations.

Acknowledgements: The authors wish to thank the *CONICET* (*National Research Council of Argentina*), *ANPCyT* (*National Agency for Scientific and Technological Promotion, Argentina*), and *UNS* (*Universidad Nacional del Sur*, Bahía Blanca, Argentina) for financial support.

Received: December 30, 2009; Revised: March 23, 2010; Published online: DOI: 10.1002/mats.200900096

Keywords: bivariate distributions; inversion methods; modeling; polymerization; probability generating functions

[1] G. J. Wells, W. H. Ray, *Macromol. Mater. Eng.* **2005**, *290*, 319.
[2] P. Pladis, C. Kiparissides, *Chem. Eng. Sci.* **1998**, *53*, 3315.
[3] W. H. Ray, *Macromolecules* **1971**, *4*, 162.
[4] W. H. Ray, T. L. Douglas, E. W. Godsalve, *Macromolecules* **1971**, *4*, 166.
[5] A. Krallis, D. Meimaroglou, C. Kiparissides, *Chem. Eng. Sci.* **2008**, *63*, 4342.
[6] D. Meimaroglou, A. Krallis, V. Saliakas, C. Kiparissides, *Macromolecules* **2007**, *40*, 2224.
[7] A. Krallis, C. Kiparissides, *Chem. Eng. Sci.* **2007**, *62*, 5304.
[8] S. Kumar, D. Ramkrishna, *Chem. Eng. Sci.* **1996**, *51*, 1311.
[9] R. A. Hutchison, *Macromol. Theory Simul.* **2001**, *10*, 144.
[10] C. Schmidt, M. Busch, D. Lilge, M. Wulkow, *Macromol. Mater. Eng.* **2005**, *290*, 404.
[11] L. Christov, G. Georgiev, *Macromol. Theory Simul.* **1995**, *4*, 177.
[12] C. Kiparissides, *J. Process Control* **2006**, *16*, 205.
[13] M. Asteasuain, C. Sarmoria, A. Brandolin, *Polymer* **2002**, *43*, 2513.
[14] M. Asteasuain, A. Brandolin, C. Sarmoria, *Polymer* **2002**, *43*, 2529.
[15] M. Asteasuain, C. Sarmoria, A. Brandolin, *Polymer* **2002**, *43*, 2363.
[16] M. Asteasuain, C. Sarmoria, A. Brandolin, *J. Appl. Polym. Sci.* **2003**, *88*, 1676.
[17] M. Asteasuain, A. Brandolin, C. Sarmoria, *Polymer* **2004**, *45*, 321.
[18] M. Asteasuain, M. Soares, M. K. Lenzi, M. Cunningham, C. Sarmoria, J. C. Pinto, A. Brandolin, *Macromol. React. Eng.* **2007**, *1*, 622.
[19] M. Asteasuain, A. Brandolin, *Comput. Chem. Eng.* **2008**, *32*, 396.
[20] M. Asteasuain, M. Soares, M. K. Lenzi, R. A. Hutchinson, M. Cunningham, A. Brandolin, J. C. Pinto, C. Sarmoria, *Macromol. React. Eng.* **2008**, *2*, 414.
[21] M. Asteasuain, A. Brandolin, *Macromol. React. Eng.* **2009**, *3*, 398.
[22] P. P. Valkó, J. Abate, *Appl. Numer. Math.* **2005**, *53*, 73.
[23] A. Brandolin, M. Asteasuain, C. Sarmoria, A. R. López, K. S. Whiteley, B. del Amo Fernández, *Polym. Eng. Sci.* **2001**, *41*, 1156.
[24] C. de Boor, "*A Practical Guide to Splines*", Springer, New York 1978.